Multi-omics insights into the microbial oxidation of seawater-soluble crude oil components

Yina Liu [‖,†,×,#,*], Helen K. White [‡], Rachel L. Simister [‡], David Waite [§], Shelby L. Lyons [‡], Elizabeth B. Kujawinski [‖]

[‖] Department of Marine Chemistry & Geochemistry, Woods Hole Oceanographic Institution, Woods Hole, Massachusetts, United States

[†] Geochemical and Environmental Research Group, Texas A&M University, College Station, Texas, United States

[×] Department of Oceanography, Texas A&M University, College Station, Texas, United States

[‡] Department of Chemistry, Haverford College, Haverford, Pennsylvania, United States

[§] School of Biological Sciences, University of Auckland, Auckland, New Zealand

* Corresponding author: Yina Liu, yina.l.liu@gmail.com

Present address: Geochemical and Environmental Research Group, Texas A&M University, College Station, Texas, United States

16 TOC Art

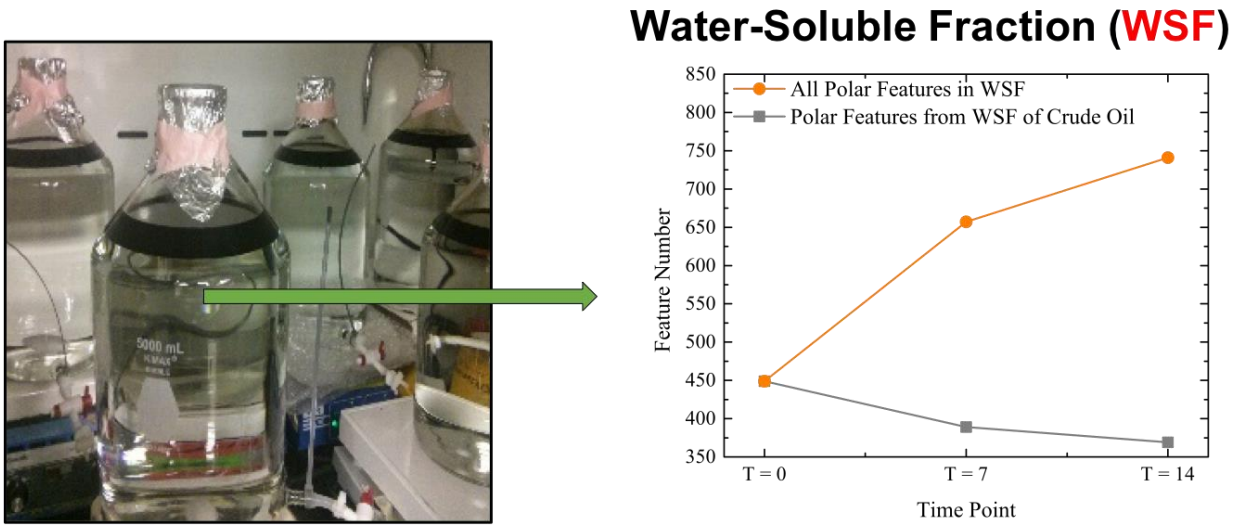

17

18

19

ABSTRACT

Studies assessing the environmental impacts of oil spills focus primarily on the non-water-soluble components, leaving the fate of the water-soluble fraction (WSF) largely unexplored. In this study, we combined chemical and genomic analyses to examine the degradation of crude oil WSF in seawater in the absence of light in a laboratory experiment. Over a 14-day incubation period, microbes transformed WSF into various metabolic intermediates, without a significant change in dissolved organic carbon concentrations. Microbial transformation processes increased the chemical diversity and overall oxygen content of WSF compounds, consistent with an increase in dioxygenase gene abundances. The majority of metabolites formed from the transformation of WSF could not be structurally identified with existing databases, but elemental formulas suggest that many of these compounds could be oxidation products of water-soluble non-polar compounds such as PAHs. In particular, O3 metabolites may represent a key transition point for WSF degradation. Salicylic acid (O3) is labile to generalist marine bacteria, and its dynamics and gene products likely provide a route for complete WSF remineralization. The environmental persistence and toxicity of WSF metabolic products are still unknown, but results from this study provide a framework for further exploration of the fate of WSF in marine ecosystems.

INTRODUCTION

Millions of barrels of crude oil are released to the ocean each year from unintentional spillages and natural seepage.[1] A small, but significant, fraction of the oil dissolves in the water and behaves differently than the bulk oil. The composition of dissolved oil is distinct from the total oil and is enriched in small (<1000 Da), polar molecules.[2, 3] Despite decades of study on the fate of oil in the environment, the water-soluble fraction (WSF) is vastly understudied because its components are not resolved in traditional gas-chromatography-based analytical methods. Consequently, we know much less about the factors affecting the fate and transport of crude oil WSF in marine ecosystems, despite evidence suggesting that this fraction is enriched during weathering and is more toxic to aquatic organisms than the parent oil.[4-7]

The best-studied oil spill occurred at the *Deepwater Horizon* (DWH) drill site in 2010, where 3.19 million barrels of oil spilled into the Gulf of Mexico over a period of 87 days,[8] making it the largest offshore oil spill in U.S. history.[9-12] Unlike many major oil spills, crude oil from the Macondo well was injected into the water column from the deep sea. A widespread neutrally buoyant subsurface plume, as thick as 200 m, was observed at 1100 m depth and persisted for months after the blowout.[9] Assessments during the early response estimated that water-soluble crude oil components were preferentially enriched in this subsurface plume,[13] with water-soluble hydrocarbons such as low molecular weight n-alkanes and monoaromatic hydrocarbons comprising ~69% by mass.[9, 12, 14] The preferential enrichment of crude oil WSF in the deep ocean underscores dissolution as an important process driving the distribution of spilled DWH oil.[13] Similar enhancements are expected at any oil-water interface, such as oil slicks in surface water or terrestrial spills.

In response to the DWH spill, numerous studies examined the fate, ecotoxicological impacts, and degradation of the released oil.[13, 15-21] For example, microbial composition and oil degradation pathways deduced from genome sequences and transcripts were investigated in diverse impacted environments, e.g. the oil plume, deep-sea sediments, and oiled beaches.[14, 19, 20, 22-24] These studies often have a focus on biologically mediated chemical transformations and degradation of major compound classes in crude oils, such as n-alkanes, monoaromatic compounds (benzene, toluene, ethylene, and xylene, or BTEX), and polycyclic aromatic hydrocarbons (PAHs).[15, 25-27] Absent from these studies, however, is information on the microbial response specific to the subset of crude oil that is truly dissolved in water and more polar than hydrocarbons, i.e. compounds that contain heteroatoms (N, S, and O). Early response assessments during the DWH spill suggested that polar compounds accounted for ~10% of the spilled oil by mass, or ~0.41 million barrels of largely uncharacterized polar crude oil.[13] These compounds are not routinely monitored in oil studies, because they are not readily accessible with traditional gas chromatography (GC)-based analytical methods; thus, the chemical characteristics, fate, and transport of polar compounds during DWH could not be included in early responses.[13]

Polar compounds account for < 15% by mass in bulk crude oil, [28] but may account for a substantial fraction (70-82%) of the water-soluble fraction (WSF), [4, 29] depending on the oil type and weathering extent. Recent studies examining the dissolution of crude and weathered oils in seawater have improved understanding of the chemical composition of WSF.[2, 3, 30] Compounds containing NSO preferentially partition into seawater. [2, 3] These NSO-containing compounds are more polar than hydrocarbons and appear to be resistant to degradation and toxic to organisms.[4, 13] For example, uncharacterized compounds from WSF fractions generated from microbial degradation of crude oil were found to be toxic to marine organisms (Crustacea),[6] highlighting the

critical gap in understanding WSF chemical composition and its biogeochemical transformations in the context of ecotoxicity. The microbial response to WSF, however, is relatively unexplored, particularly in comparison to BTEX,[31, 32] PAHs,[33, 34] and alkanes[24, 31]. During the DWH spill, next-generation genomic techniques were employed to examine the sequential dominance of hydrocarbon degraders in conjunction with traditional and emerging assessments of oil degradation, but these tools were unable to link directly to WSF chemistry. [14, 17, 20, 35]

Complex mixture analysis enabled by advanced mass spectrometry methods can provide valuable information on the composition and fate of spilled oils, particularly the polar fraction contained in WSF. Ultrahigh resolution mass spectrometry such as Fourier transform ion cyclotron resonance mass spectrometry (FT-ICR MS) was widely used in response to the DWH spill, in order to obtain insight into crude oil-derived compounds that could not be resolved with GC-based methods.[2, 25, 26, 30, 36] When applied to biological systems, these techniques identify and quantify metabolites produced by organisms, thus providing metabolite profiles of microbial cultures or communities under various conditions.[22, 25] In this study, we combined metabolite profiling (i.e. metabolomics) and metagenomics methods to examine the evolving chemical signature of WSF and the dynamics of polar crude oil compounds within dark aerobic incubations with natural seawater bacterial consortia. This approach combined with existing knowledge of hydrocarbon degradation pathways enabled us to explore the microbial mechanisms responsible for WSF degradation in aerobic seawater, analogous to oxic waters such as the surface ocean and the DWH subsurface plume.[37]

EXPERIMENTAL SECTION

Incubation Experiment. We created WSF by slow dissolution of Macondo oil surrogate (source crude oil – MC252; Item IDs A0067V and A0067X) in filter-sterilized Vineyard Sound seawater (VSW), following the low energy mixing methods described in Liu and Kujawinski[2] (Supporting Information and Figure S1a). Briefly, we loaded the Macondo oil surrogate on the surface of VSW at a 5:95 (v/v) ratio and allowed the oil dissolution to occur over 7 days in dark at room temperature. Low energy was applied to ensure exchange across the water column, but no oil droplets were entrained into the water. This method confined oil dissolution at the upper water column of the vessel and the limited mixing provided a mean of dilution from upper to lower water column, which mimicked the dilution of oil components across the concentration gradient in the aquatic environment. After 7 days, we filtered the resulting water-accommodated fraction (WAF) through a 0.7 μm glass fiber GF/F filter to collect the final, truly water-soluble oil component (i.e. WSF). This method captures primarily low molecular weight PAHs and polar, water-soluble compounds, because volatile hydrocarbons such as benzene, toluene, ethylbenzene, and xylene (BTEX) will be lost over the 7-day mixing period as well as during the filtration process. The dissolved organic carbon (DOC) concentration of WSF was comparable to that observed in the field during DWH spill (Figures S3).[38]

We established three parallel treatments, each in triplicate, to explore microbial community changes in response to the addition of crude oil-derived components in the WSF (Figures S1b): (1) the VSW control, which contained background seawater dissolved organic matter (DOM) and natural bacterial consortia; (2) the succinic acid treatment, which contained seawater DOM, succinic acid, and natural bacterial consortia; and (3) the WSF treatment, which contained seawater DOM, crude oil WSF, and natural bacterial consortia. Succinic acid was used as a simple carbon substrate control to distinguish opportunistic microbes responding to carbon addition,[39] relative to

128 microbes responding uniquely to WSF components. In treatments (2) and (3), we added the organic
129 substrates at similar DOC concentrations (succinic acid = 347 ± 7 μM-C; WSF 311 ± 7 μM-C).
130 We added filter-sterilized ammonium chloride (NH_4Cl; 4 nM) and sodium phosphate (NaH_2PO_4;
131 0.3 nM) to all incubation chambers to mitigate nutrient limitation for cell growth. We inoculated
132 each treatment with natural bacterial consortia at a volume ratio of 10%, at the beginning of the
133 experiment (Supporting Information). One liter of headspace remained in each incubation
134 chamber, and we maintained aerobic conditions by swirling the incubation chambers gently three
135 times daily. We kept all incubations in the dark at room temperature (~24ºC) throughout the 14-
136 day experiment. The experiment was conducted in the dark to minimize photo-oxidation;[15, 40]
137 consequently, the observed chemical signatures over the experiment should be due primarily to
138 heterotrophic transformations. Details on the experiment setup are provided in the Supporting
139 Information.
140 **Sample Collection, Preparation, and Analyses.** We collected samples on three days (0, 7, 14).
141 On the sampling day, we swirled each bottle gently to ensure homogeneity and then filtered each
142 sample through a 0.2-μm Omnipore (Millipore Sigma) membrane filter under low vacuum.
143 Filtrates were used for external metabolite profiling, PAH analysis, and dissolved organic carbon
144 (DOC) analysis. We used microbial biomass retained on the filter for 16S rRNA gene and
145 metagenomics analyses. We enumerated bacteria in 10 mL of unfiltered water that was fixed with
146 borate-buffered formalin (2% final concentration) and frozen at -20°C. Our WSF protocol includes
147 GF/F filtration to remove oil droplets[2] and thus we do not expect significant amounts of
148 hydrophobic or sparingly hydrophilic compounds to be retained on the 0.2-μm membrane filters
149 used for biomass collection. We stored the filters at -80°C until extraction.

We acidified the filtrates (2L) to pH ~3 immediately after filtration, extracted the samples with PPL solid-phase extraction (SPE) cartridges (Bond Elut, Agilent), and then eluted with 100% methanol as described in Dittmar et al.[41] and modified by Longnecker.[42] The eluents were stored at -20°C until mass spectrometry analysis. Immediately before analysis, we dried down the eluents to near dryness, and reconstituted them in 250 μL of 95:5 water:acetonitrile. We added deuterated biotin (5 μL; final concentration 0.05 μg/mL) to each sample as an internal standard. PPL resins preferentially capture the aromatic compounds in WSF, but do not retain very small, highly polar molecules such as succinic acid.[43] Therefore, to ensure similar extracted carbon concentrations across all treatments and within the pooled samples, we diluted the WSF treatment eluents 50× due to high concentrations of extracted carbon relative to the non-WSF treatments. We combined 50 μL of each sample to create a pooled sample as a reference for data quality control and processing.

We divided all samples into two equal volumes, one for targeted analysis and one for untargeted analysis, following methods described by Kido Soule et al.[44] The untargeted approach, using liquid chromatography coupled to FT-ICR MS (LC-FT-ICR MS) equipped with an electrospray ionization (ESI) source, allows examination of metabolite profiles without prior knowledge of sample composition, and thus enables simultaneous identification of known compounds and discovery of previously unknown metabolites. Metabolite profiles from different incubation conditions at the three time points provided valuable information on how the microbes transformed WSF components compared to other organic substrates over the 14-day experiment. Here, we define a metabolite profile as all the features in a given sample, where a feature is defined as a unique combination of mass to charge ratio (*m/z*) and retention time (RT). Each feature corresponds to a specific metabolite or to a group of co-eluting isomers.

We subjected the top four features in each mass scan to tandem mass spectrometry (MS/MS or MS2) for compound identification. We applied rigorous data quality control procedures to ensure data robustness, e.g. removing features whose variability is driven by instrumental parameters and/or are consistently present in all samples at similar intensities (see Supporting Information). After these measures, approximately 40-48% of features in the dataset had associated MS2 spectra. We used a step-wise approach to classify metabolites of interests based on the Metabolomics Standards Initiative's (MSI) established four-level standard.[45] Specifically, a level-4 classification includes unknown features that passed QA/QC but do not match any literature and database values; a level-3 putative characterization requires a match between observed exact mass values and elemental formulas; and a level-2 putative annotation requires a multi-component match between exact mass and other physicochemical properties (e.g. RT and/or fragmentation pattern) with literature or external libraries. The highest confidence level-1 identification requires at least two of four independent confirmations of RT, exact mass, MS2 spectrum, or isotope patterns from a chemical standard under identical analytical conditions.[45] We used the MetFrag *in silico* tool[46] to search the fragmentation patterns and exact mass values to generate level-2 putative annotations. We compared the search results with metabolites listed in Kyoto Encyclopedia of Genes and Genomes (KEGG) for key hydrocarbon degradation pathways. For pathways with multiple level-2 putative annotations, we searched our feature list for level-3 putative characterizations within these pathways. We assigned elemental formulas for the level-3 features using an automated compound identification algorithm (CIA) as described in Kujawinski and Behn[47] with parameters from Liu and Kujawinski.[2] We did not consider pathways with only level-3 putative characterizations, due to the inability to distinguish among structural isomers with the same mass. Finally, we confirmed level-1 identities of key metabolites with commercial standards, including

six intermediates related to degradation of naphthalene and methylnaphthalenes, namely 3- and 4-hydroxybenzaldehyde, salicylic acid, 3- and 4-methylsalicylic acid, and gentistic acid. These metabolites were then quantified by LC triple-quadrupole-MS (see Supporting Information).

It should be noted that many observed features could not be identified with literature or database searches (i.e. level-4). Additionally, many level-2 and level-3 features do not have commercial standards available. Due to the lack of appropriate standards for most of the detected features, feature intensities obtained with the untargeted method could not be converted to absolute concentrations. Instead, we used relative abundances to compare concentration changes among samples. We calculated relative abundance as: Σ(Intensity of feature groups)/ Σ(Intensity of all detected features) × 100, where feature groups can be defined as specific compound classes or those that contained elements of interest such as oxygen.

Compounds ionizable by ESI contain at least one polar function group; thus, features detected by LC-FT-ICR MS are, by analytical definition, more polar than hydrocarbons containing no polar functional groups. Therefore, we equate polar compounds with those observed within the LC-FT-ICR MS analytical window in the subsequent discussions.

Sample Collection for PAH Analysis. We extracted 100 mL of WSF samples with dichloromethane (DCM) for PAH analysis. We dried the extracts with anhydrous Na_2SO_4 and removed excess DCM by rotary evaporation. We reconstituted the concentrated samples with toluene for global chemical characterization through direct infusion FT-ICR MS (data not shown). We took aliquots of ~250 μL from the remaining samples in toluene and performed solvent exchange by drying down the toluene under a gentle stream of high purity nitrogen. The dried samples were shipped to Haverford College for PAH analysis. The samples were reconstituted with DCM before analysis by gas chromatography mass spectrometry (GC-MS). We expect that

our PAH concentrations are underestimates due to the sample drying steps. For example, naphthalene was not detected, which is inconsistent with this oil's known composition.[48] From previous work, we expect the less volatile PAHs should account for ~10% of the WSF.[4] Individual PAH analyzed in this study included: naphthalene, C1-C4 alkylated naphthalenes, biphenyl, fluorene, C1-C3 alkylated fluorenes, dibenzothiophene, C1-C3 alkylated dibenzothiophenes, anthracene, C1-alkylated anthracene, phenanthrene, C1-C3 alkylated phenanthrenes, chrysene, C1-C3alkylated chrysenes, and triphenylene and benzo(a)anthracene. Detailed method for PAH analysis is described in the Supporting Information.

16S rRNA Gene and Metagenomics Analysis. We extracted microbial DNA from all filters using the MO BIO PowerWater (PW) kit (MOBIO Laboratories, Inc., Carlsbad, CA), according to the manufacturer's instructions. Purified genomic DNA was submitted to the University of Wisconsin-Madison Biotechnology Center. Further details of sample preparations for 16S rRNA gene and metagenomics sequencing, library construction and bioinformatics analysis are provided in Supporting Information.

RESULTS AND DISCUSSION

Presence of WSF Selected for Distinct Microbial Communities. Both chemical and microbial community compositions within the same treatment type changed between the initial time point and 7 and/or 14 days (Figures S2a and b), indicating selection of microbial community based on the organic substrates and microbial alteration of the organic compounds in the starting incubation media. Among the three treatments, the chemical and microbial community compositions were different between non-WSF (i.e. VSW and succinic acid) and WSF incubations (Figures S2a and b). The use of succinic acid as a control carbon source allowed us to determine that this observed

shift in microbial community is due specifically to the addition of WSF and not due to opportunistic microbes. Indeed, we observed known hydrocarbon degraders uniquely in the WSF treatment, including *Cycloclasticus*, *Oceaniserpentilla*, and *Rhodospirillales*, consistent with field observations of microbial diversity during the DWH spill (Table S5 and S6).[14, 24, 49]

WSF is Transformed in Incubation Experiments. We used changes in DOC concentrations across time points to evaluate complete remineralization of organic carbon to CO_2 in each treatment. DOC values were not statistically significantly different across the 14-day incubation in the WSF treatments, based on a one-way ANOVA test at 95% confidence level (Figure S3). In contrast, DOC concentrations decreased more than 100 μM-C by T = 14 in the succinic acid treatment, suggesting catabolism of succinate for energy (Figure S3). DOC concentrations in the VSW treatment were also not statistically significantly different across the three time points, which was likely due to the overall lower biomass and microbial activity as a result of lower DOC concentrations (Figures S4).

We used LC-FT-ICR MS to examine detailed chemical changes as the microbes altered WSF. We define polar WSF-derived chemical features (P-WSF_{Total}), resolved by LC-FT-ICR MS, to be those found in WSF treatment but not in any non-WSF treatments. We culled the list of features to those that were found in all replicates at a time point. We then divided P-WSF_{Total} into P-WSF_0, or the polar WSF compounds found at T = 0, and P-WSF_M, or the polar metabolites produced during microbial degradation of WSF compounds (Figure S5).

To understand the chemical dynamics within WSF over the course of our experiment, we further subdivided P-WSF_0 into four groups: P-$WSF_{0\text{-}C}$, or features that were likely **c**onsumed completely (present only at T = 0); P-$WSF_{0\text{-}U}$, or features that were **u**naltered (similar relative abundance values over 14 days); P-$WSF_{0\text{-}I}$, or features whose relative abundances **i**ncreased over 14 days; and

P-$WSF_{0\text{-}D}$, or features whose relative abundances **d**ecreased over 14 days. The last three groups (P-$WSF_{0\text{-}U}$, P-$WSF_{0\text{-}I}$, and P-$WSF_{0\text{-}D}$) include features present in WSF treatment samples at all time points. We based our feature classifications on pair-wise one-tailed Student's t-test of feature intensities. A visual overview of our classification scheme is shown in Figure S5.

Overall, the features in P-WSF_{Total} increased from 449 at T = 0 to 741 at T = 14 (Figure 1; Table S1), indicating formation of new compounds as a result of microbial transformation of WSF crude oil. Only 80 of 449 (<18 %) P-WSF_0 features were missing by the end of the experiment, due either to complete degradation or to reduction below the detection limit (Figure 1; Table S1). In contrast, P-WSF_M accounted for 41% and 50% of the total features observed in T = 7 and 14, respectively (Tables S1 and S2). The similarity in DOC concentrations in WSF treatment samples across time points, together with the increase in the number of P-WSF_{Total} and the small fraction of P-$WSF_{0\text{-}C}$, implies that the majority of compounds initially found in WSF were transformed into metabolic intermediates by microbial degradation rather than completely remineralized to CO_2, within the time frame of the experiment.

Changes in the relative abundances of features in P-$WSF_{0\text{-}I}$ and P-$WSF_{0\text{-}D}$ were significant between T = 0 and T = 7 but not significant between T = 7 and T = 14, based on paired one-tailed Student's t-tests (Figure 2 and Table S3). In contrast, increases in relative abundances for P-WSF_M features were significant between T= 0 and T = 7, and between T = 7 and T = 14 (Figure 2 and Table S3). These findings suggest that processes that lead to a decrease or increase in abundances of P-WSF_0 features proceed at slower rates, or not at all, after T = 7; while production of P-WSF_M continues after T = 7 and potentially beyond T = 14. The source of P-WSF_M may be P-WSF_0 and/or low-molecular weight, water-soluble non-polar compounds, such as PAHs. We can discount the first possibility because the change in relative abundance in P-$WSF_{0\text{-}D}$ is minimal between T = 7

and T = 14. In contrast, the second possibility could only be explained by microbial oxidation of compounds that were originally outside the LC-FT-ICR MS analytical window, such as the non-polar compounds in WSF.

Degradation of PAHs is a Likely Source of Polar Metabolites in WSF. One of the possible sources of P-WSF_M is the oxidation of non-polar compounds. To investigate whether non-polar compounds in WSF are the sources of polar compounds, we focused our data interpretation on the degradation of water-soluble PAHs, i.e. typically those with less than 3-rings, which should account for ~10% of the WSF.[4] If all or a major fraction of PAHs were completely remineralized into CO_2, such a process should result in statistically significant changes in DOC concentrations. However, DOC concentrations did not change significantly while total PAH concentration decreased and the number of P-WSF_{Total} increased (Figures 1 and S6). These observations support the notion that the source of the increasing P-WSF_M was likely the non-polar compounds that were not detected by LC-FT-ICR MS at T = 0.

We identified a total of 56 metabolites that occur within known aromatic compound degradation pathways, such as xylene, toluene, naphthalenes, and PAHs with three or fewer rings (Table S4). Twenty-four of the 56 compounds from P-WSF_{Total} were assigned a level-2 putative annotation based on exact mass and fragmentation pattern matches (Table S4). Of the 24 Level-2 metabolites, 7 were associated with the degradation of naphthalene and methyl-naphthalenes (Table S4), even though naphthalene was not detected in PAH analysis. Multiple naphthalene degradation products were observed across all time points with either negligible abundances at T = 0 and elevated abundances at T=7 and/or T=14 or with the highest abundances at T = 7 (e.g. Figures S7 and S8). We observed multiple metabolites from the degradation of aromatic compounds with 1-3 rings, but no metabolites associated with the degradation of high molecular weight PAHs. This is

consistent with the absence of high molecular weight PAHs in WSF based on their low aqueous solubilities.[2]

O3 and O4 Metabolites are Important Intermediates in WSF Transformations. The number of putatively annotated compounds related to WSF degradation accounted for only a small percentage (<12%) of P-WSF_{Total} in each sample. To better understand the characteristics of the broad range of compounds observed in WSF, existing chemical reaction information available in the KEGG database and metagenomics data from this study was used to guide the interpretation of the remaining P-WSF_{Total} features.

We focused on P-WSF_{Total} features with assigned formulas (Levels 1, 2, and 3) that contained oxygen atoms, since oxidation is a well-known mechanism for oil degradation. Aerobic biodegradation of PAHs is catalyzed by either monooxygenases or dioxygenases, enzymes that add one or two oxygen atoms, respectively, in the initial steps.[34, 50-53] In bacteria, dioxygenases are the primary enzymes that initiate the PAH degradation.[34, 51, 54] For PAHs with three or fewer rings, dioxygenase-catalyzed oxygen addition occurs up to O4, at which point one ring opens. The open-ring O4 intermediates break down into compounds with higher oxygen to carbon ratios, such as O3 and O4 attached to only one aromatic ring (Figure 3). For example, degradation of naphthalene initiated via the naphthalene 1,2-dioxygenase pathway produces metabolic intermediates with oxygen numbers as follows: O0 → O2 (two isomers) → O4 → O4 (one ring opens) → O2 (lower ring number) → O3 → O4 (towards central metabolism) (Figure 3).

In this experiment, three O3 compounds, salicylic and 3- and 4-methylsalicylic acids, were the most abundant Level-1 metabolic intermediates (Table S4 and Figure S7). These compounds, however, only account for a small fraction of the DOC (<0.1%), suggesting that: (1) a large

proportion of the WSF compounds were unknown and (2) these compounds likely represent a pool of WSF organic carbon that has low concentrations but high flux.

To further examine oxygen-containing compounds beyond the level-1 identification, we compared the oxygen distributions of compounds with $C_xH_yO_z$ formulas. Comparisons of relative abundance between each oxygen compound class across time points were based on pair-wise one-tailed Student's t-test. Within the oxygen number distributions of P-WSF_{Total} features, the relative abundances of O4 compounds were significantly higher at T = 7 and 14 than T = 0 (Figure 4a). Changes in relative abundance of P-$WSF_{0\text{-}I}$ features show that most of the production occurred in the O3 and O4 classes (Figure 4b). The relative abundance of O3 P-WSF_M also increased significantly at T = 14, compared to T = 7 (Figure 4d). The oxygen number distribution characteristics from a broader range of compounds in P-WSF_{Total} features are similar to known PAH degradation pathways. Therefore, the high relative abundance of O4 compounds in WSF is likely due to multiple reactions from the degradation of polar and non-polar compounds.

The observed oxygen number pattern and complementary genomics data suggest that the degradation of naphthalene and other PAHs in the experiment was likely attributed to dioxygenase-catalyzed reactions. We observed enrichments of multiple genes encoding for dioxygenases in the WSF samples (Figure 5). Although evidence of monooxygenase-catalyzed PAH metabolism is present in some bacteria, [31, 55] such reactions are predominantly observed in eukaryotic cells such as fungi, yeast, and mammalian cells.[56-59] Unlike dioxygenase-encoding genes, we did not observe genes that encode for monooxygenases. The increase in O3 class relative abundance was, therefore, not related to monooxygenases, and is instead more likely to be breakdown products from O4 compounds after the first ring opens. We found that both P-$WSF_{0\text{-}I}$ and P-WSF_M features include many O3 compounds (Figure 4b and d). The high abundance of O3 compounds may reflect

the production and accumulation of intermediates similar to salicylic acids (i.e. salicylic acid, its methylated forms, and other modifications), which are key metabolites from naphthalene and methyl-naphthalene degradation. Interestingly, the abundance of a subset of O3 compounds also decreased substantially over the course of the experiment within P-$WSF_{0\text{-}D}$ (Figure 4c), suggesting some of these compounds were rapidly degraded. These findings suggest that the O3 compound class is a dynamic group of compounds with production, accumulation, and degradation occurring simultaneously.

O3 Metabolites Such as Salicylic Acids Represent a Key Transition Point for WSF Degradation. Salicylic acid is a metabolic intermediate in multiple PAH degradation pathways such as naphthalene, anthracene, fluorene, and phenanthrene; thus, it is reasonable to assume that the degradation of naphthalene, anthracene, fluorene, and phenanthrene in WSF all contributed to the observed concentration of salicylic acid in this study. The methylated forms of salicylic acid (3- and 4-methylsalicylic acids) are key metabolic intermediates in the degradation of 1- and 2-methylnaphthalenes, respectively.

The salicylaldehyde dehydrogenase gene (*nahF*, (KEGG, K00152)), which encodes the enzyme that catalyzes the formation of salicylic acid in the naphthalene degradation pathway,[60, 61] was enriched in the WSF treatments (Figure 5). Further degradation of salicylic acid can proceed via numerous mechanisms, depending on microbial community composition and their associated genes.[62] For example, in the naphthalene degradation pathway, salicylic acid is transformed into one of two different products through competing reaction mechanisms, i.e. gentistic acid and catechol. We detected trace amounts of gentistic acid in WSF samples (Figure S7), but not catechol. Furthermore, the gene encoding the enzyme for converting salicylic acid to catechol, namely salicylate hydroxylase (*nahG*, (KEGG, K00480)), was not enriched in the WSF samples.

Interestingly, the *nahG* gene was elevated in non-WSF samples relative to the WSF treatments (Figure 5), particularly in the VSW treatment. The enrichment of *nahG* gene in the VSW treatment suggest some of the bacteria in seawater retain the genetic capacity to metabolize salicylic acid through the catechol pathway, even though the concentration of salicylic acid in seawater was low. This finding suggests that while the production of salicylic acid via PAH degradation pathways may require specific hydrocarbon-degrading microbial groups, i.e. those that thrive in the presence of WSF, removal of salicylic acid may be mediated by generalist non-oil degrading bacteria. This finding underscores the importance of community structure and succession in complete oil degradation. It is known that during the DWH oil spill, distinct groups of oil-degrading microbes bloomed at different stages of the oil spill.[18] These microbes potentially produced an array of metabolites that could be utilized by the general microbial community as carbon sources. We propose that while specialized microbes initiate the degradation of WSF, the activity of generalists may be important for the full remineralization of WSF compounds to CO_2. Interestingly, salicylic acid has been shown to enhance the degradation of high molecular weight PAHs, [34, 63-66] raising the intriguing possibility that salicylic acid stimulates and facilitates degradation of PAHs.

CONCLUSIONS

WSF represents an important component of spilled oil that can play a role in ecotoxicology, and can impact ecosystems, [4, 6, 67] e.g. in subsurface plume of DWH and in the water column beneath a surface oil slick (Figure 6). The molecular-level understanding of the fate of the polar compounds in crude oil WSF, however, is still scarce. This study offers the first multi-omics insights into microbial degradation of WSF, achieved by integrating a broad suite of chemical features with hydrocarbon-degrading genes.

Although this is a controlled laboratory experiment, our results set important reference frames for future oil spill studies and provide new compound targets for field monitoring. The wide range of oxygen-containing WSF compounds share similar oxygen number distributions as those from the degradation of PAHs through dioxygenase pathways. Intermediate metabolites with three oxygen atoms may represent an important transition point in oil degradation in nature. We hypothesize that O3 metabolites such as salicylic acids are funneling compounds for microbial degradation of hydrocarbons. Initial degradation steps may require specialized microbes, but the subsequent metabolism of intermediate products could be achieved by a more diverse group of microbes present in seawater microbial consortia. Consistent with our laboratory findings, we detected salicylic acids and gentistic acid in archived field samples collected in the DWH plume (Table S7), suggesting these compounds may be used as markers for PAH degradation in the field. Additional work with fresh samples or surface oil slicks is needed to confirm these results. Nevertheless, our results highlight the complexity of uncharacterized polar compounds in WSF and their transformation products. The ecotoxicity of this complex pool remains poorly constrained, underscoring the need for improved understanding of the fate and ecotoxicity of WSF on long and short timescales. With more comprehensive knowledge of WSF and its degradation products, markers for assessing the fate and ecotoxicity of spilled oil in the environment can be developed.

AUTHOR INFORMATION

Corresponding Author

* Yina Liu

Present Addresses

Present address: Geochemical and Environmental Research Group (GERG), Texas A&M University, College Station, TX 77845.

Author Contributions

The manuscript was written through contributions of all authors. All authors have given approval to the final version of the manuscript. The authors declare no competing financial interest.

Supporting Information. Additional experimental details, figures and tables as noted in the text. This material is available free of charge via the Internet at http://pubs.acs.org.

Funding Sources. This study is funded by the Gulf of Mexico Research Initiative (GOMRI) Project # 161684 to EBK and HKW.

ACKNOWLEDGMENTS

We would like to thank M. Kido Soule for her assistance in the FT-ICR-MS facility, K. Longnecker for her assistance in data processing. G. Swarr and W. Johnson for their help with the extraction efficiency experiment. Data presented in this manuscript is freely available online: doi:10.7266/N71C1TTK (nutrients and TOC data), doi:10.7266/N7N29TW0 (targeted metabolomics data), doi:10.7266/N7WM1BBP (non-targeted metabolomics data), and doi10.7266/N7W95762 (metagenomic data).

ABBREVIATIONS.

FT-ICR-MS, Fourier transform ion cyclotron resonance mass spectrometry; VSW, Vineyard Sound seawater; WSF, water-soluble fraction; OTU, operational taxonomic unit; DOC, dissolved organic carbon. WAF, water-accommodated fraction, DOM, dissolved organic matter.

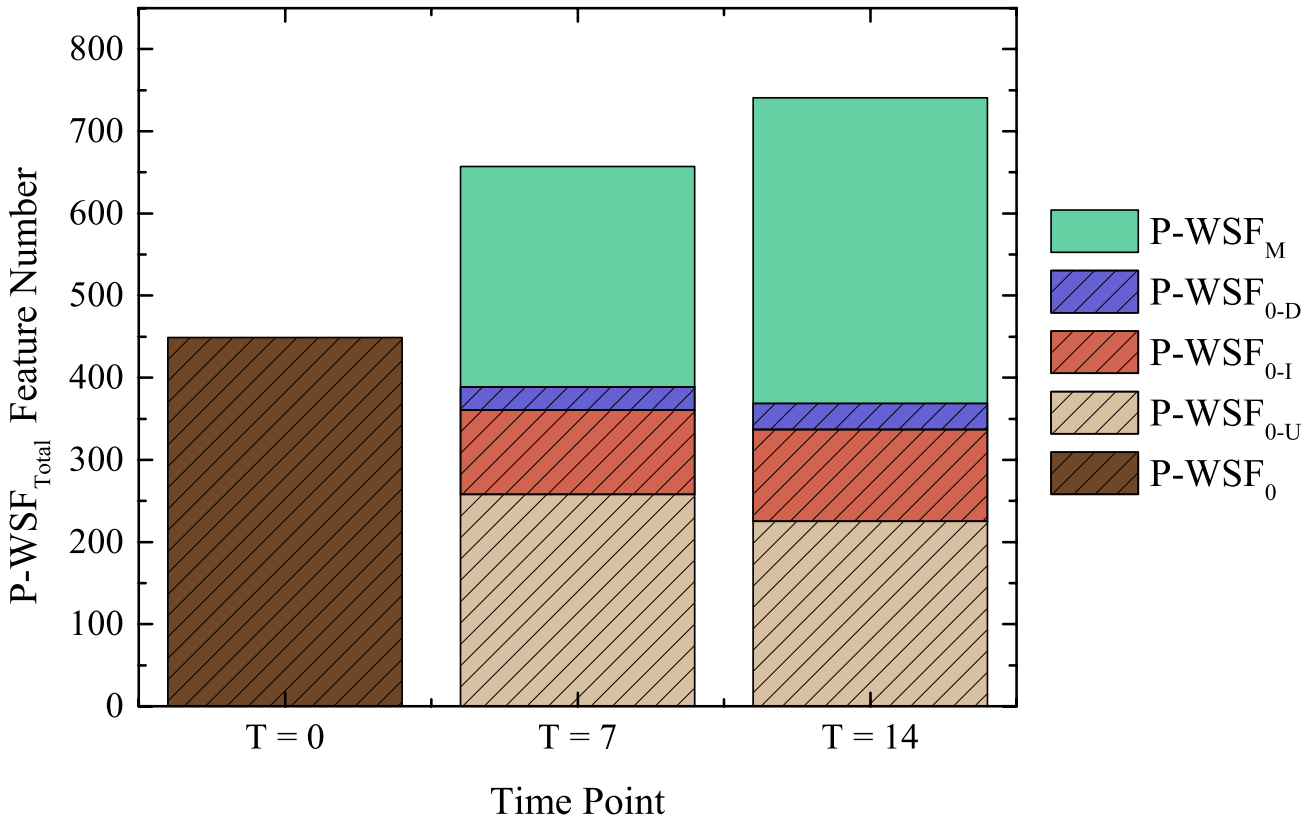

Figure 1. Number of observed features across time points T = 0, T = 7, and T = 14 for $P\text{-}WSF_{Total}$. All features shown here were present in all treatment replicates of a time point. Compounds derived from WSF of crude oil at T = 0 ($P\text{-}WSF_0$) are indicated with stripes. Dark brown striped bar represents $P\text{-}WSF_0$ features in the starting material of the incubation experiment. Light brown striped bars highlighted features that persisted from T = 0 to T = 14 and whose relative abundance did not change ($P\text{-}WSF_{0\text{-}U}$). Red striped bars highlighted features whose relative abundance increased over the course of the experiment ($P\text{-}WSF_{0\text{-}I}$). Blue striped bars highlighted features whose relative abundance decreased the course of the experiment ($P\text{-}WSF_{0\text{-}D}$). Green bars highlighted new compounds present at T = 7 and T = 14, but not at T = 0 ($P\text{-}WSF_M$). The difference between the initial striped bar and the sum of the three striped bars at T=7 and T=14 constitutes the features that were lost ($P\text{-}WSF_{0\text{-}C}$).

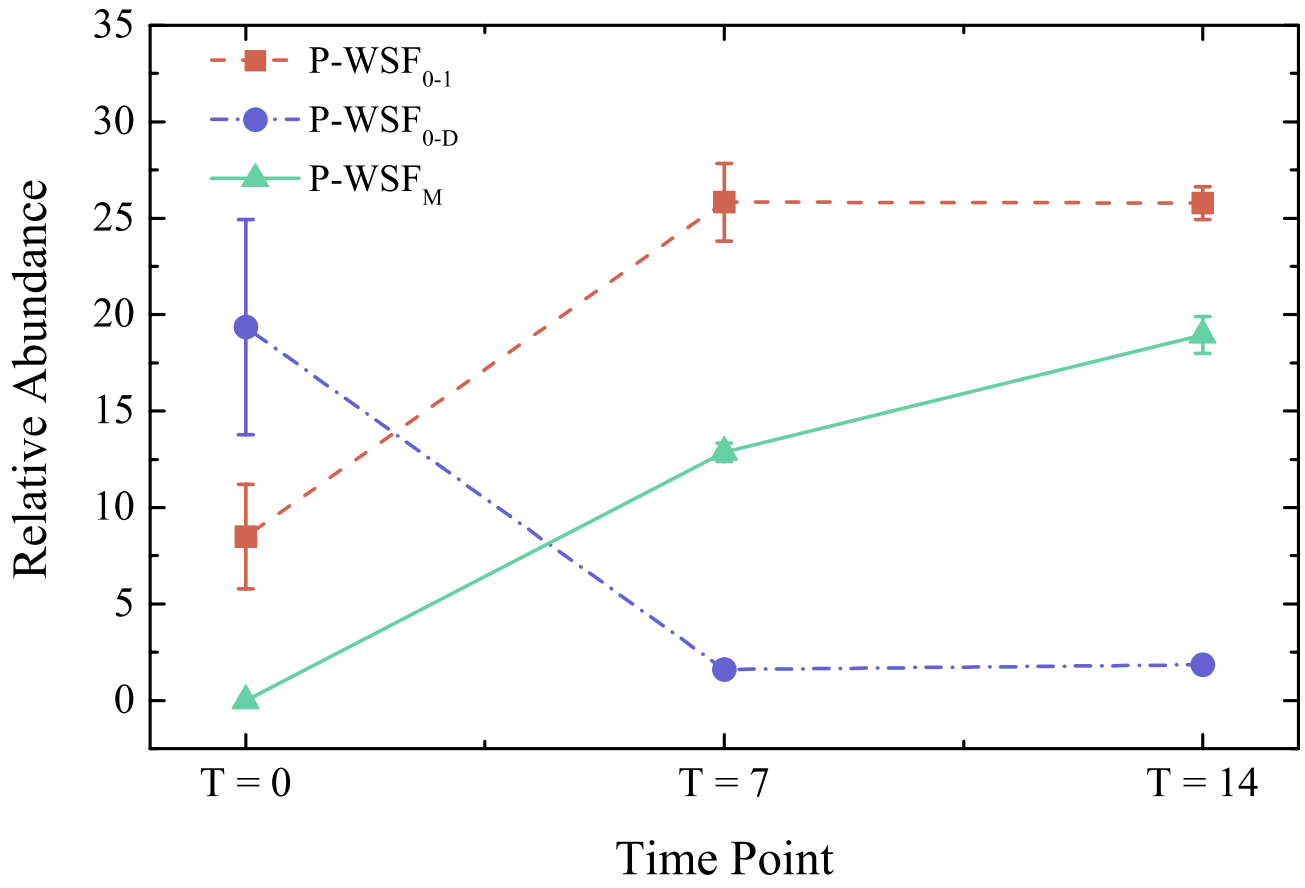

462

463 **Figure 2.** Relative abundance of three compound groups observed in WSF treatment (P-WSF$_0$):
464 P-WSF$_{0\text{-}I}$ (red squares), P-WSF$_{0\text{-}D}$ (blue circles), P-WSF$_M$ (green triangles). Error bars represent
465 one standard deviation (n = 3) of relative intensity in each compound class at each time point.

466

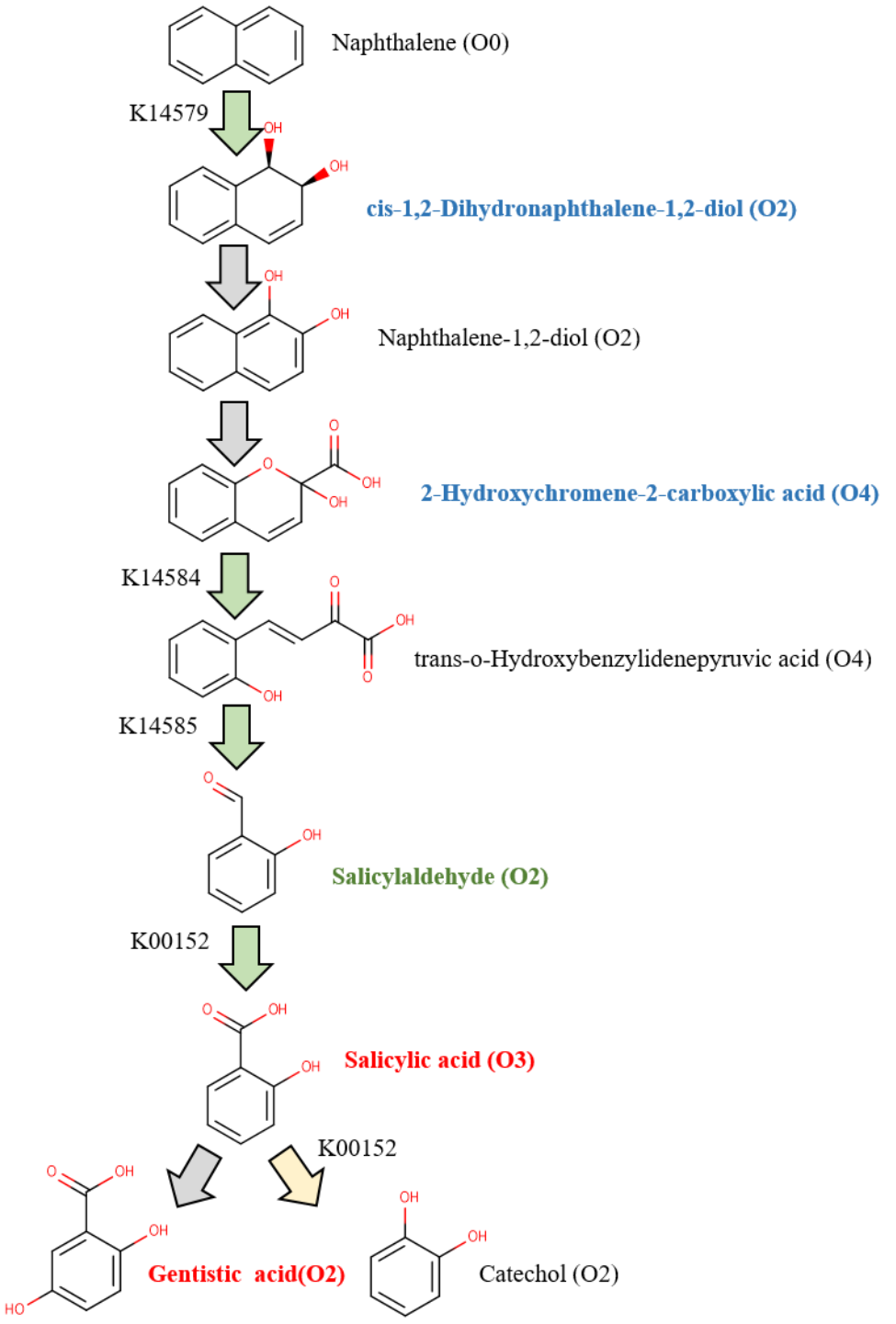

Figure 3. Metabolic pathway of naphthalene degradation initiated through a dioxygenase, based on KEGG. Green arrows indicate the presence of the coding gene encoded in our samples. Grey arrows indicate absence of the coding gene in this study. A yellow arrow indicates the coding gene was observed but not enriched in WSF treatment samples. Chemical names for each structure was labeled with oxygen number indicated in parenthesis. Chemical names in red indicate a level-1 identification. Chemical names in green indicate a level-2 putative annotation. Chemical names in

474 blue indicate a level-3 putative characterization. Chemical names in black indicated that we did
475 not observe these compounds. BLAST identities of dioxygenase genes detected against an
476 experimentally validated database[68] are listed in Table S12.

477

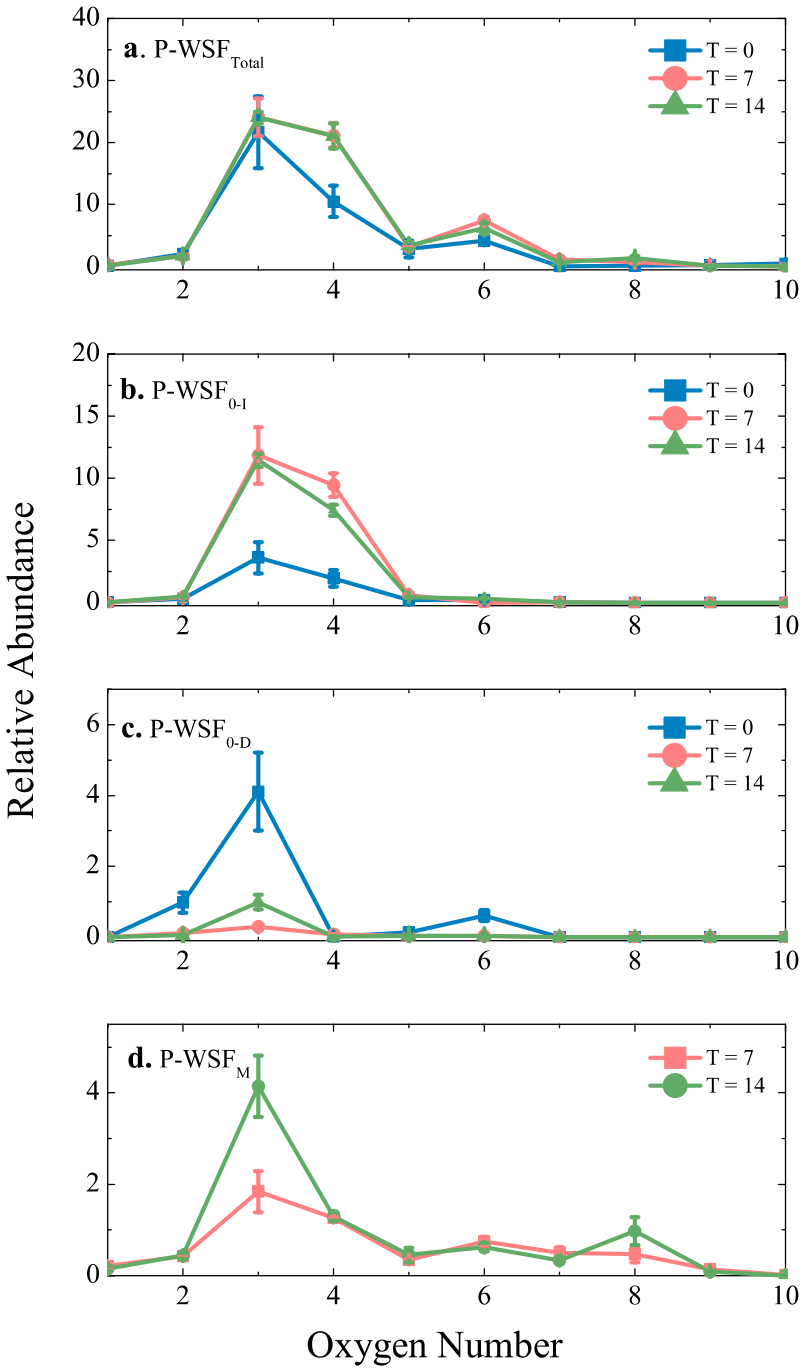

Figure 4. Oxygen number distributions of $C_xH_yO_z$ compounds observed in WSF. (a) P-WSF$_{Total}$, (b) P-WSF$_{0\text{-}I}$, (c) P-WSF$_{0\text{-}D}$, and (d) P-WSF$_M$ in the three time-points (T = 0 in blue, T = 7 in red, and T = 14 in green). Error bars indicate one standard deviation around the mean of triplicate analyses.

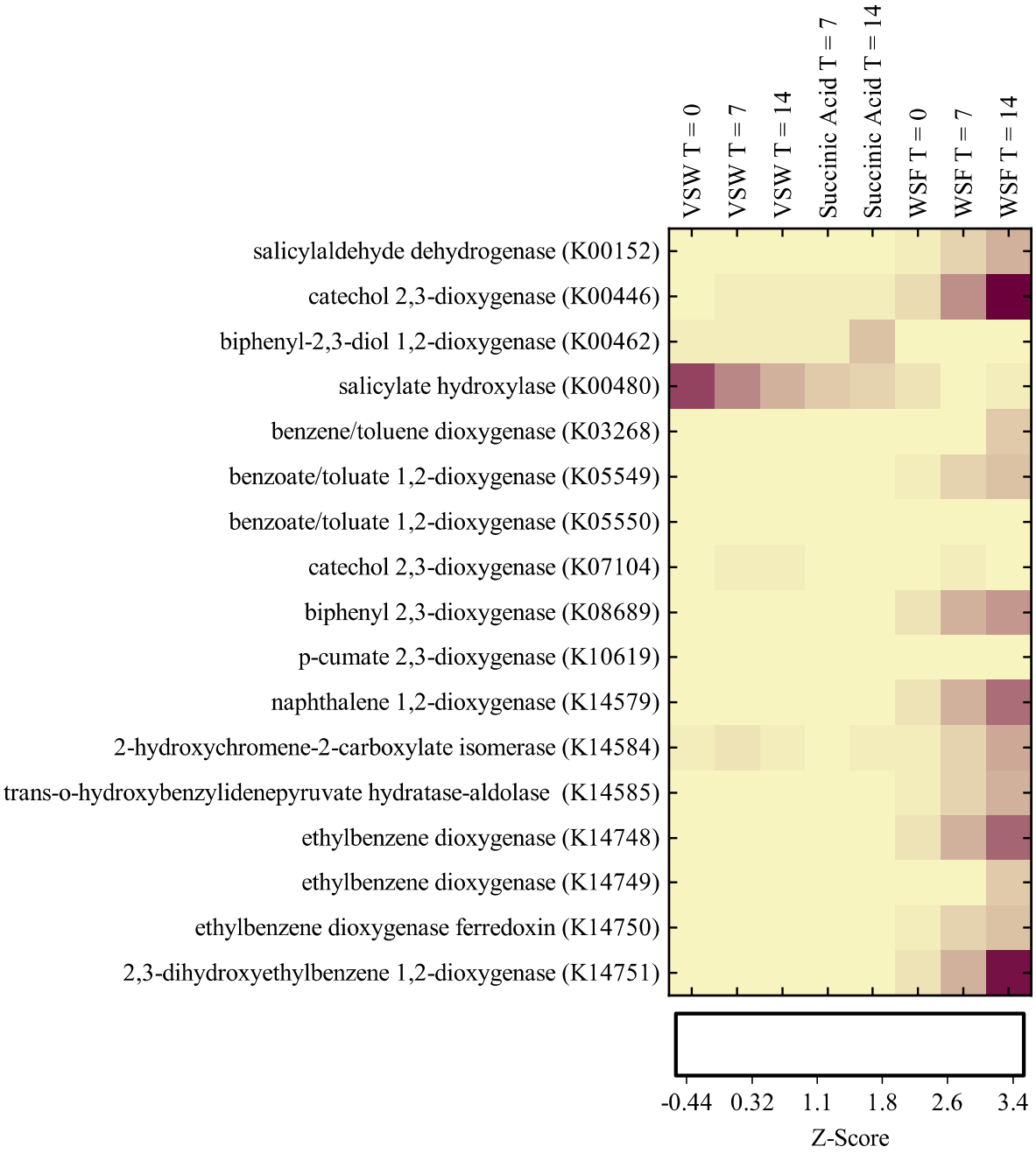

485

486 **Figure 5.** Heatmap of genes that encode for aromatic compound metabolisms identified using
487 metagenomic analysis (described in Supporting Information). Only genes encoding for the
488 degradation of oil-derived compounds are included. The darker color indicates higher Z-Score
489 values for specific genes compared to the light yellow. Abundance and percentile of the gene are
490 listed in Table S11. BLAST identities of dioxygenase genes detected against an experimentally
491 validated database[68] are listed in Table S12.

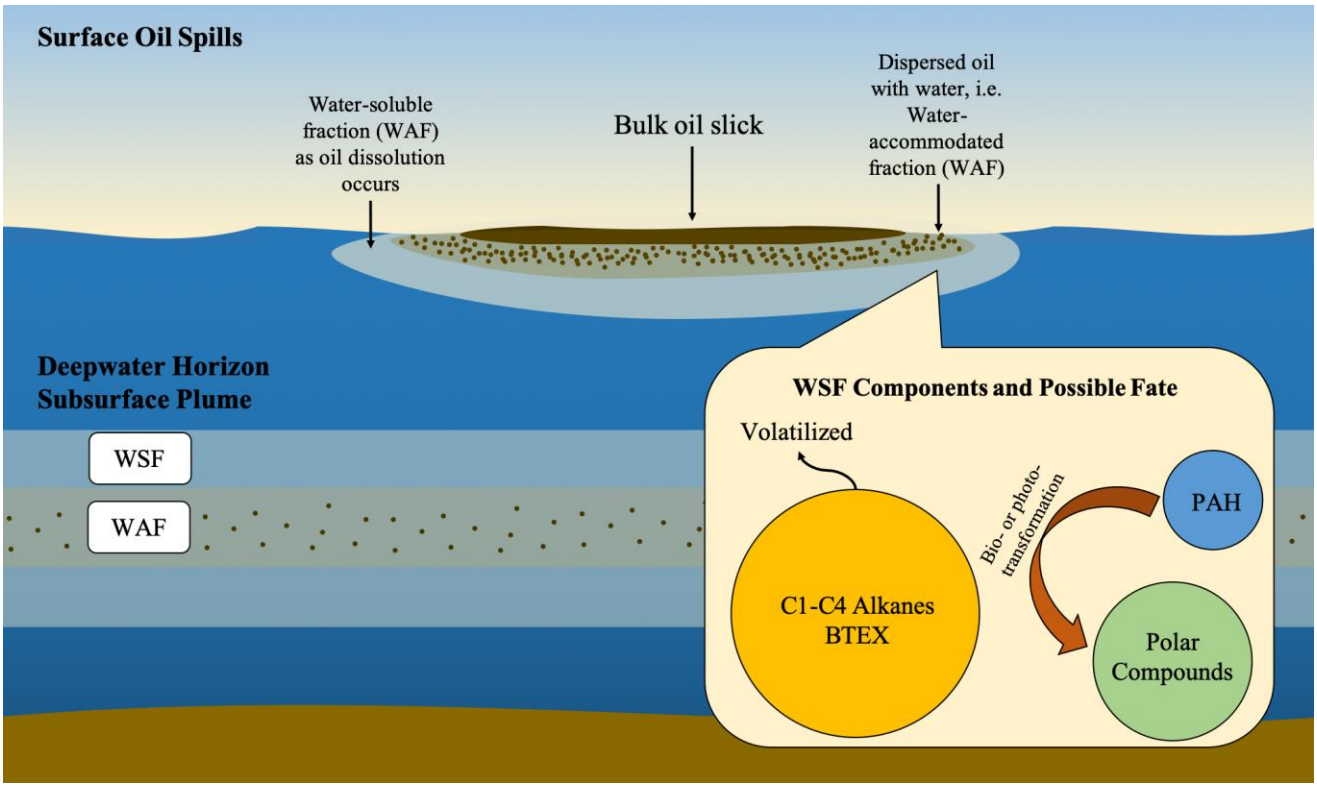

Figure 6. Proposed occurrence and fate of the water-soluble fraction (WSF) in the environment. Through dissolution, WSF is expected in the water around the surface oil slicks during an aquatic oil spill. The chemical fingerprint of WSF is distinct from the water-accommodated fraction (WAF), which contained emulsified oil droplets. During the DWH oil spill, we postulate both WAF and WSF were present in the subsurface plume. In the water column, WSF is expected to contain a larger fraction of BTEX, low molecular weight PAHs, and polar compounds. Based on our results, non-polar compounds such as BTEX and PAHs can contribute to polar compounds in WSF through bio-transformation in the water column. At the surface, BTEX may readily volatilize while PAHs are transformed to polar compounds through photo- and bio-mediated pathways.

503 REFERENCE
504
505 1. National Research Council, *Oil in the Sea Iii:Inputs, Fates, and Effects*. The National
506 Academies Press: Washington, DC, 2003.

507 2. Liu, Y.; Kujawinski, E. B., Chemical Composition and Potential Environmental Impacts
508 of Water-Soluble Polar Crude Oil Components Inferred from ESI FT-ICR MS. *PLoS ONE* **2015,**
509 *10* (9), e0136376.

510 3. Stanford, L. A.; Kim, S.; Klein, G. C.; Smith, D. F.; Rodgers, R. P.; Marshall, A. G.,
511 Identification of Water-Soluble Heavy Crude Oil Organic-Acids, Bases, and Neutrals by
512 Electrospray Ionization and Field Desorption Ionization Fourier Transform Ion Cyclotron
513 Resonance Mass Spectrometry. *Environ Sci Technol* **2007,** *41* (8), 2696-2702.

514 4. Melbye, A. G.; Brakstad, O. G.; Hokstad, J. N.; Gregersen, I. K.; Hansen, B. H.; Booth,
515 A. M.; Rowland, S. J.; Tollefsen, K. E., Chemical and Toxicological Characterization of an
516 Unresolved Complex Mixture-Rich Biodegraded Crude Oil. *Environmental Toxicology and*
517 *Chemistry* **2009,** *28* (9), 1815-1824.

518 5. Barron, M. G.; Carls, M. G.; Short, J. W.; Rice, S. D., Photoenhanced Toxicity of Aqueous
519 Phase and Chemically Dispersed Weathered Alaska North Slope Crude Oil to Pacific Herring Eggs
520 and Larvae. *Environmental Toxicology and Chemistry* **2003,** *22* (3), 650-660.

521 6. Shelton, M. E.; Chapman, P. J.; Foss, S. S.; Fisher, W. S., Degradation of Weathered Oil
522 by Mixed Marine Bacteria and the Toxicity of Accumulated Water-Soluble Material to Two
523 Marine Crustacea. *Archives of Environmental Contamination and Toxicology* **1999,** *36* (1), 13-20.

524 7. Maki, H.; Sasaki, T.; Harayama, S., Photo-Oxidation of Biodegraded Crude Oil and
525 Toxicity of the Photo-Oxidized Products. *Chemosphere* **2001,** *44* (5), 1145-1151.

526 8. Prince, R. C.; Atlas, R. M., Bioremediation of Marine Oil Spills. *Consequences of*
527 *Microbial Interactions with Hydrocarbons, Oils, and Lipids: Biodegradation and Bioremediation*
528 **2018**, 1-25.

529 9. Camilli, R.; Reddy, C. M.; Yoerger, D. R.; Van Mooy, B. A. S.; Jakuba, M. V.; Kinsey,
530 J. C.; McIntyre, C. P.; Sylva, S. P.; Maloney, J. V., Tracking Hydrocarbon Plume Transport and
531 Biodegradation at Deepwater Horizon. *Science* **2010,** *330* (6001), 201-204.

532 10. Joye, S. B., Deepwater Horizon, 5 Years On. *Science* **2015,** *349* (6248), 592-593.

533 11. McNutt, M. K.; Camilli, R.; Crone, T. J.; Guthrie, G. D.; Hsieh, P. A.; Ryerson, T. B.;
534 Savas, O.; Shaffer, F., Review of Flow Rate Estimates of the Deepwater Horizon Oil Spill.
535 *Proceedings of the National Academy of Sciences* **2012,** *109* (50), 20260-20267.

536 12. Ryerson, T. B.; Camilli, R.; Kessler, J. D.; Kujawinski, E. B.; Reddy, C. M.; Valentine,
537 D. L.; Atlas, E.; Blake, D. R.; de Gouw, J.; Meinardi, S.; Parrish, D. D.; Peischl, J.; Seewald,

538 J. S.; Warneke, C., Chemical Data Quantify Deepwater Horizon Hydrocarbon Flow Rate and
539 Environmental Distribution. *Proceedings of the National Academy of Sciences* **2012**.

540 13. Reddy, C. M.; Arey, J. S.; Seewald, J. S.; Sylva, S. P.; Lemkau, K. L.; Nelson, R. K.;
541 Carmichael, C. A.; McIntyre, C. P.; Fenwick, J.; Ventura, G. T.; Van Mooy, B. A. S.; Camilli,
542 R., Composition and Fate of Gas and Oil Released to the Water Column During the Deepwater
543 Horizon Oil Spill. *Proceedings of the National Academy of Sciences* **2012,** *109* (50), 20229-20234.

544 14. Valentine, D. L.; Kessler, J. D.; Redmond, M. C.; Mendes, S. D.; Heintz, M. B.; Farwell,
545 C.; Hu, L.; Kinnaman, F. S.; Yvon-Lewis, S.; Du, M.; Chan, E. W.; Tigreros, F. G.; Villanueva,
546 C. J., Propane Respiration Jump-Starts Microbial Response to a Deep Oil Spill. *Science* **2010,** *330*
547 (6001), 208-211.

548 15. Aeppli, C.; Carmichael, C. A.; Nelson, R. K.; Lemkau, K. L.; Graham, W. M.; Redmond,
549 M. C.; Valentine, D. L.; Reddy, C. M., Oil Weathering after the Deepwater Horizon Disaster Led
550 to the Formation of Oxygenated Residues. *Environ Sci Technol* **2012,** *46* (16), 8799-8807.

551 16. Spier, C.; Stringfellow, W. T.; Hazen, T. C.; Conrad, M., Distribution of Hydrocarbons
552 Released During the 2010 MC252 Oil Spill in Deep Offshore Waters. *Environmental Pollution*
553 **2013,** *173*, 224-230.

554 17. Kleindienst, S.; Seidel, M.; Ziervogel, K.; Grim, S.; Loftis, K.; Harrison, S.; Malkin, S.
555 Y.; Perkins, M. J.; Field, J.; Sogin, M. L.; Dittmar, T.; Passow, U.; Medeiros, P. M.; Joye, S.
556 B., Chemical Dispersants Can Suppress the Activity of Natural Oil-Degrading Microorganisms.
557 *Proceedings of the National Academy of Sciences* **2015,** *112* (48), 14900-14905.

558 18. Dubinsky, E. A.; Conrad, M. E.; Chakraborty, R.; Bill, M.; Borglin, S. E.; Hollibaugh,
559 J. T.; Mason, O. U.; M. Piceno, Y.; Reid, F. C.; Stringfellow, W. T.; Tom, L. M.; Hazen, T.
560 C.; Andersen, G. L., Succession of Hydrocarbon-Degrading Bacteria in the Aftermath of the
561 Deepwater Horizon Oil Spill in the Gulf of Mexico. *Environ Sci Technol* **2013,** *47* (19), 10860-
562 10867.

563 19. Hazen, T. C.; Dubinsky, E. A.; DeSantis, T. Z.; Andersen, G. L.; Piceno, Y. M.; Singh,
564 N.; Jansson, J. K.; Probst, A.; Borglin, S. E.; Fortney, J. L.; Stringfellow, W. T.; Bill, M.;
565 Conrad, M. E.; Tom, L. M.; Chavarria, K. L.; Alusi, T. R.; Lamendella, R.; Joyner, D. C.;
566 Spier, C.; Baelum, J.; Auer, M.; Zemla, M. L.; Chakraborty, R.; Sonnenthal, E. L.; D'haeseleer,
567 P.; Holman, H.-Y. N.; Osman, S.; Lu, Z.; Van Nostrand, J. D.; Deng, Y.; Zhou, J.; Mason, O.
568 U., Deep-Sea Oil Plume Enriches Indigenous Oil-Degrading Bacteria. *Science* **2010,** *330* (6001),
569 204-208.

570 20. Mason, O. U.; Hazen, T. C.; Borglin, S.; Chain, P. S. G.; Dubinsky, E. A.; Fortney, J.
571 L.; Han, J.; Holman, H.-Y. N.; Hultman, J.; Lamendella, R.; Mackelprang, R.; Malfatti, S.;
572 Tom, L. M.; Tringe, S. G.; Woyke, T.; Zhou, J.; Rubin, E. M.; Jansson, J. K., Metagenome,
573 Metatranscriptome and Single-Cell Sequencing Reveal Microbial Response to Deepwater Horizon
574 Oil Spill. *ISME J* **2012,** *6* (9), 1715-1727.

21. Incardona, J. P.; Vines, C. A.; Anulacion, B. F.; Baldwin, D. H.; Day, H. L.; French, B. L.; Labenia, J. S.; Linbo, T. L.; Myers, M. S.; Olson, O. P.; Sloan, C. A.; Sol, S.; Griffin, F. J.; Menard, K.; Morgan, S. G.; West, J. E.; Collier, T. K.; Ylitalo, G. M.; Cherr, G. N.; Scholz, N. L., Unexpectedly High Mortality in Pacific Herring Embryos Exposed to the 2007 Cosco Busan Oil Spill in San Francisco Bay. *Proceedings of the National Academy of Sciences* **2012,** *109* (2), E51-E58.

22. Kimes, N. E.; Callaghan, A. V.; Aktas, D. F.; Smith, W. L.; Sunner, J.; Golding, B.; Drozdowska, M.; Hazen, T. C.; Suflita, J. M.; Morris, P. J., Metagenomic Analysis and Metabolite Profiling of Deep–Sea Sediments from the Gulf of Mexico Following the Deepwater Horizon Oil Spill. *Frontiers in Microbiology* **2013,** *4*, 50.

23. Kostka, J. E.; Prakash, O.; Overholt, W. A.; Green, S. J.; Freyer, G.; Canion, A.; Delgardio, J.; Norton, N.; Hazen, T. C.; Huettel, M., Hydrocarbon-Degrading Bacteria and the Bacterial Community Response in Gulf of Mexico Beach Sands Impacted by the Deepwater Horizon Oil Spill. *Appl. Environ. Microbiol.* **2011,** *77* (22), 7962-7974.

24. Redmond, M. C.; Valentine, D. L., Natural Gas and Temperature Structured a Microbial Community Response to the Deepwater Horizon Oil Spill. *Proceedings of the National Academy of Sciences* **2012,** *109* (50), 20292-20297.

25. Seidel, M.; Kleindienst, S.; Dittmar, T.; Joye, S. B.; Medeiros, P. M., Biodegradation of Crude Oil and Dispersants in Deep Seawater from the Gulf of Mexico: Insights from Ultra-High Resolution Mass Spectrometry. *Deep Sea Research Part II: Topical Studies in Oceanography* **2016,** *129*, 108-118.

26. Chen, H.; Hou, A.; Corilo, Y. E.; Lin, Q.; Lu, J.; Mendelssohn, I. A.; Zhang, R.; Rodgers, R. P.; McKenna, A. M., 4 Years after the Deepwater Horizon Spill: Molecular Transformation of Macondo Well Oil in Louisiana Salt Marsh Sediments Revealed by Ft-Icr Mass Spectrometry. *Environ Sci Technol* **2016**.

27. Aeppli, C.; Nelson, R. K.; Radović, J. R.; Carmichael, C. A.; Valentine, D. L.; Reddy, C. M., Recalcitrance and Degradation of Petroleum Biomarkers Upon Abiotic and Biotic Natural Weathering of Deepwater Horizon Oil. *Environ Sci Technol* **2014,** *48* (12), 6726-6734.

28. Hughey, C. A.; Rodgers, R. P.; Marshall, A. G.; Qian, K.; Robbins, W. K., Identification of Acidic Nso Compounds in Crude Oils of Different Geochemical Origins by Negative Ion Electrospray Fourier Transform Ion Cyclotron Resonance Mass Spectrometry. *Organic Geochemistry* **2002,** *33* (7), 743-759.

29. Siron, R.; Rontani, J. F.; Giusti, G., Chemical Characterization of a Water Soluble Fraction (WSF) of Crude Oil. *Toxicological & Environmental Chemistry* **1987,** *15* (3), 223-229.

30. Ray, P. Z.; Chen, H.; Podgorski, D. C.; McKenna, A. M.; Tarr, M. A., Sunlight Creates Oxygenated Species in Water-Soluble Fractions of Deepwater Horizon Oil. *J Hazard Mater* **2014,** *280* (0), 636-643.

31. Mason, O.; Han, J.; Woyke, T.; Jansson, J., Single-Cell Genomics Reveals Features of a *Colwellia* Species That Was Dominant During the Deepwater Horizon Oil Spill. *Frontiers in Microbiology* **2014,** *5*.

32. Wang, L.; Qiao, N.; Sun, F.; Shao, Z., Isolation, Gene Detection and Solvent Tolerance of Benzene, Toluene and Xylene Degrading Bacteria from Nearshore Surface Water and Pacific Ocean Sediment. *Extremophiles* **2008,** *12* (3), 335-342.

33. Kappell, A. D.; Wei, Y.; Newton, R. J.; Van Nostrand, J. D.; Zhou, J.; McLellan, S. L.; Hristova, K. R., The Polycyclic Aromatic Hydrocarbon Degradation Potential of Gulf of Mexico Native Coastal Microbial Communities after the Deepwater Horizon Oil Spill. *Frontiers in Microbiology* **2014,** *5*, 205.

34. Ghosal, D.; Ghosh, S.; Dutta, T. K.; Ahn, Y., Current State of Knowledge in Microbial Degradation of Polycyclic Aromatic Hydrocarbons (PAHs): A Review. *Frontiers in Microbiology* **2016,** *7*, 1369.

35. Kessler, J. D.; Valentine, D. L.; Redmond, M. C.; Du, M.; Chan, E. W.; Mendes, S. D.; Quiroz, E. W.; Villanueva, C. J.; Shusta, S. S.; Werra, L. M.; Yvon-Lewis, S. A.; Weber, T. C., A Persistent Oxygen Anomaly Reveals the Fate of Spilled Methane in the Deep Gulf of Mexico. *Science* **2011,** *331* (6015), 312-315.

36. Vaughan, P. P.; Wilson, T.; Kamerman, R.; Hagy, M. E.; McKenna, A.; Chen, H.; Jeffrey, W. H., Photochemical Changes in Water Accommodated Fractions of MC252 and Surrogate Oil Created During Solar Exposure as Determined by Ft-Icr Ms. *Marine Pollution Bulletin* **2016**.

37. Du, M.; Kessler, J. D., Assessment of the Spatial and Temporal Variability of Bulk Hydrocarbon Respiration Following the Deepwater Horizon Oil Spill. *Environ Sci Technol* **2012,** *46* (19), 10499-10507.

38. Zhou, Z.; Guo, L.; Shiller, A. M.; Lohrenz, S. E.; Asper, V. L.; Osburn, C. L., Characterization of Oil Components from the Deepwater Horizon Oil Spill in the Gulf of Mexico Using Fluorescence Eem and Parafac Techniques. *Mar Chem* **2013,** *148*, 10-21.

39. Nelson, C. E.; Carlson, C. A., Tracking Differential Incorporation of Dissolved Organic Carbon Types among Diverse Lineages of Sargasso Sea Bacterioplankton. *Environmental Microbiology* **2012,** *14* (6), 1500-1516.

40. Vaughan, P. P.; Wilson, T.; Kamerman, R.; Hagy, M. E.; McKenna, A.; Chen, H.; Jeffrey, W. H., Photochemical Changes in Water Accommodated Fractions of MC252 and Surrogate Oil Created During Solar Exposure as Determined by Ft-Icr Ms. *Marine Pollution Bulletin* **2016,** *104* (1), 262-268.

41. Dittmar, T.; Koch, B.; Hertkorn, N.; Kattner, G., A Simple and Efficient Method for the Solid-Phase Extraction of Dissolved Organic Matter (SPE-DOM) from Seawater. *Limnol. Oceanogr. Methods* **2008,** *6*, 230-235.

42. Longnecker, K., Dissolved Organic Matter in Newly Formed Sea Ice and Surface Seawater. *Geochim Cosmochim Ac* **2015,** *171*, 39-49.

43. Johnson, W. M.; Kido Soule, M. C.; Kujawinski, E. B., Extraction Efficiency and Quantification of Dissolved Metabolites in Targeted Marine Metabolomics. *Limnology and Oceanography: Methods* **2017**, n/a-n/a.

44. Kido Soule, M. C.; Longnecker, K.; Johnson, W. M.; Kujawinski, E. B., Environmental Metabolomics: Analytical Strategies. *Mar Chem* **2015,** *177, Part 2*, 374-387.

45. Sumner, L. W.; Amberg, A.; Barrett, D.; Beale, M. H.; Beger, R.; Daykin, C. A.; Fan, T. W. M.; Fiehn, O.; Goodacre, R.; Griffin, J. L.; Hankemeier, T.; Hardy, N.; Harnly, J.; Higashi, R.; Kopka, J.; Lane, A. N.; Lindon, J. C.; Marriott, P.; Nicholls, A. W.; Reily, M. D.; Thaden, J. J.; Viant, M. R., Proposed Minimum Reporting Standards for Chemical Analysis. *Metabolomics* **2007,** *3* (3), 211-221.

46. Ruttkies, C.; Schymanski, E. L.; Wolf, S.; Hollender, J.; Neumann, S., Metfrag Relaunched: Incorporating Strategies Beyond in Silico Fragmentation. *Journal of Cheminformatics* **2016,** *8* (1), 3.

47. Kujawinski, E. B.; Behn, M. D., Automated Analysis of Electrospray Ionization Fourier Transform Ion Cyclotron Resonance Mass Spectra of Natural Organic Matter. *Analytical Chemistry* **2006,** *78* (13), 4363-4373.

48. Pelz, O.; Brown, J.; Huddleston, M.; Rand, G.; Gardinali, P.; Stubblefield, W.; BenKinney, M. T.; Ahnell, A.; Bp Gcro, H.; Exponent, M., Selection of a Surrogate MC252 Oil as a Reference Material for Future Aquatic Toxicity Tests and Other Studies. *survival* **2011,** *20*, 25-000.

49. Hazen, T. C.; Dubinsky, E. A.; Desantis, T. Z.; Andersen, G. L.; Piceno, Y. M.; Singh, N.; Jansson, J. K.; Probst, A.; Borglin, S. E.; Fortney, J. L.; Stringfellow, W. T.; Bill, M.; Conrad, M. E.; Tom, L. M.; Chavarria, K. L.; Alusi, T. R.; Lamendella, R.; Joyner, D. C.; Spier, C.; Baelum, J.; Auer, M.; Zemla, M. L.; Chakraborty, R.; Sonnenthal, E. L.; D'Haeseleer, P.; Holman, H. Y.; Osman, S.; Lu, Z.; Van Nostrand, J. D.; Deng, Y.; Zhou, J.; Mason, O. U., Deep-Sea Oil Plume Enriches Indigenous Oil- Degrading Bacteria. *Science* **2010,** *330*.

50. Kelley, I.; Freeman, J.; Cerniglia, C., Identification of Metabolites from Degradation of Naphthalene by a *Mycobacterium Sp*. *Biodegradation* **1990,** *1* (4), 283-290.

51. Cerniglia, C. E., Biodegradation of Polycyclic Aromatic Hydrocarbons. *Current Opinion in Biotechnology* **1993,** *4* (3), 331-338.

52. Eaton, R. W., Organization and Evolution of Naphthalene Catabolic Pathways: Sequence of the DNA Encoding 2-Hydroxychromene-2-Carboxylate Isomerase and Trans-O-Hydroxybenzylidenepyruvate Hydratase-Aldolase from the nah7 Plasmid. *Journal of bacteriology* **1994,** *176* (24), 7757-7762.

53. Kimes, N. E.; Callaghan, A. V.; Suflita, J. M.; Morris, P. J., Microbial Transformation of the Deepwater Horizon Oil Spill – Past, Present, and Future Perspectives. *Frontiers in Microbiology* **2014,** *5*.

54. Eaton, R. W.; Chapman, P. J., Bacterial Metabolism of Naphthalene: Construction and Use of Recombinant Bacteria to Study Ring Cleavage of 1,2-Dihydroxynaphthalene and Subsequent Reactions. *Journal of Bacteriology* **1992,** *174* (23), 7542-7554.

55. Ressler, B. P.; Kneifel, H.; Winter, J., Bioavailability of Polycyclic Aromatic Hydrocarbons and Formation of Humic Acid-Like Residues During Bacterial Pah Degradation. *Appl Microbiol Biotechnol* **1999,** *53* (1), 85-91.

56. Cerniglia, C.; Crow, S., Metabolism of Aromatic Hydrocarbons by Yeasts. *Archives of Microbiology* **1981,** *129* (1), 9-13.

57. Cerniglia, C.; Freeman, J. P.; Evans, F., Evidence for an Arene Oxide-nih Shift Pathway in the Transformation of Naphthalene to 1-Naphthol by *Bacillus Cereus*. *Archives of Microbiology* **1984,** *138* (4), 283-286.

58. Jerina, D. M.; Daly, J. W., Arene Oxides: A New Aspect of Drug Metabolism. *Science* **1974,** *185* (4151), 573-582.

59. Syed, K.; Doddapaneni, H.; Subramanian, V.; Lam, Y. W.; Yadav, J. S., Genome-to-Function Characterization of Novel Fungal P450 Monooxygenases Oxidizing Polycyclic Aromatic Hydrocarbons (Pahs). *Biochemical and Biophysical Research Communications* **2010,** *399* (4), 492-497.

60. Kiyohara, H.; Nagao, K., The Catabolism of Phenanthrene and Naphthalene by Bacteria. *Microbiology* **1978,** *105* (1), 69-75.

61. Evans, W. C.; Fernley, H. N.; Griffiths, E., Oxidative Metabolism of Phenanthrene and Anthracene by Soil Pseudomonads. The Ring-Fission Mechanism. *Biochemical Journal* **1965,** *95* (3), 819-831.

62. Monticello, D. J.; Bakker, D.; Schell, M.; Finnerty, W. R., Plasmid-Borne Tn5 Insertion Mutation Resulting in Accumulation of Gentisate from Salicylate. *Appl. Environ. Microbiol.* **1985,** *49* (4), 761-764.

63. Weissenfels, W. D.; Beyer, M.; Klein, J.; Rehm, H. J., Microbial Metabolism of Fluoranthene: Isolation and Identification of Ring Fission Products. *Appl Microbiol Biotechnol* **1991,** *34* (4), 528-535.

64. Juhasz, A. L.; Naidu, R., Bioremediation of High Molecular Weight Polycyclic Aromatic Hydrocarbons: A Review of the Microbial Degradation of Benzo[a]Pyrene. *International Biodeterioration & Biodegradation* **2000,** *45* (1), 57-88.

65. Chen, S.-H.; Aitken, M. D., Salicylate Stimulates the Degradation of High-Molecular Weight Polycyclic Aromatic Hydrocarbons by Pseudomonas Saccharophila P15. *Environ Sci Technol* **1999,** *33* (3), 435-439.

66. Rentz, J. A.; Alvarez, P. J. J.; Schnoor, J. L., Benzo[a]Pyrene Degradation by Sphingomonas Yanoikuyae Jar02. *Environmental Pollution* **2008,** *151* (3), 669-677.

67. Kennedy, C. J.; Farrell, A. P., Ion Homeostasis and Interrenal Stress Responses in Juvenile Pacific Herring, *Clupea Pallasi*, Exposed to the Water-Soluble Fraction of Crude Oil. *Journal of Experimental Marine Biology and Ecology* **2005,** *323* (1), 43-56.

68. Meynet, P.; Head, I. M.; Werner, D.; Davenport, R. J., Re-Evaluation of Dioxygenase Gene Phylogeny for the Development and Validation of a Quantitative Assay for Environmental Aromatic Hydrocarbon Degraders. *FEMS microbiology ecology* **2015,** *91* (6), fiv049.